Homooligomerization of ABCA3 and its functional significance

SABRINA FRIXEL[1], AMELIE S. LOTZ-HAVLA[2], SUNČANA KERN[1], EVA KALTENBORN[1], THOMAS WITTMANN[1], SØREN W. GERSTING[2], ANIA C. MUNTAU[3], RALF ZARBOCK[1*] and MATTHIAS GRIESE[1*]

[1]German Centre for Lung Research and [2]Department of Molecular Pediatrics, Dr von Hauner Children's Hospital, Ludwig-Maximilians University, D-80337 Munich; [3]University Children's Hospital, University Medical Center Hamburg-Eppendorf, D-20246 Hamburg, Germany

Received February 9, 2016; Accepted May 11, 2016

DOI: 10.3892/ijmm.2016.2650

Abstract. ABCA3 is a surfactant lipid transporter in the limiting membrane of lamellar bodies in alveolar type II cells. Mutations in the ATP-binding cassette, sub-family A (ABC1), member 3 (*ABCA3*) gene cause respiratory distress syndrome in newborns, and chronic interstitial lung disease in children and adults. ABCA3 belongs to the class of full ABC transporters, which are supposed to be functional in their monomeric forms. Although other family members e.g., ABCA1 and ABCC7 have been shown to function as oligomers, the oligomerization state of ABCA3 is unknown. In the present study, the oligomerization of ABCA3 was investigated in cell lysates and crude membrane preparations from transiently and stably transfected 293 cells using blue native PAGE (BN-PAGE), gel filtration and co-immunoprecipitation. Additionally, homooligomerization was examined *in vivo* in cells using bioluminescence resonance energy transfer (BRET). Using BN-PAGE and gel filtration, we demonstrate that non-denatured ABCA3 exists in different oligomeric forms, with monomers (45%) and tetramers (30%) being the most abundant forms. Furthermore, we also show the existence of 20% dimers and 5% trimers. BRET analyses verified intermolecular interactions *in vivo*. Our results also demonstrated that the arrest of ABCA3 in the endoplasmic reticulum (ER), either through drug treatment or induced by mutations in *ABCA3*, inhibited the propensity of the protein to form dimers. Based on our results, we suggest that transporter oligomerization is crucial for ABCA3 function and that a disruption of oligomerization due to mutations represents a novel pathomechanism in ABCA3-associated lung disease.

Correspondence to: Professor Matthias Griese, German Centre for Lung Research, Dr von Hauner Children's Hospital, Ludwig-Maximilians University, Lindwurmstrasse 4, D-80337 Munich, Germany
E-mail: matthias.griese@med.uni-muenchen.de

*Contributed equally

Key words: diffuse parenchymal lung disease, ABC transporter, ABCA3, homooligomerization

Introduction

The ATP-binding cassette (ABC) superfamily proteins are important functional transporters in both prokaryotes and eukaryotes, which are involved in the transport of compounds across biological membranes. Almost all ABC transporters found in eukaryotes are exporters (1). In humans, the ABC family comprises 48 members (2). The abnormal function of ABC transporters has been directly linked to the causes of several human diseases, such as Tangier disease (ABCA1) (3,4), Stargardt macular dystrophy (ABCA4) (5), pseudoxanthoma elasticum (ABCC6) (6) and cystic fibrosis (ABCC7/CFTR) (7). ABC transporters have also frequently been associated with multidrug resistance in cancer chemotherapy. For example, P-glycoprotein (ABCB1) and MRP1 (ABCC1) actively efflux anticancer drugs out of cells and thus decrease their cytotoxicity (8,9).

ABC transporters share a common structure of four functional units or domains: two transmembrane domains (TMDs) and two nucleotide binding domains (NBDs) that hydrolyze ATP to provide energy for substrate transport (1). The TMDs typically contain 6 transmembrane α-helices. In eukaryotes, most ABC transporters are constituted by a single polypeptide chain containing all four functional units ('full transporters'). In the case of so-called half transporters, the functional transporter is assembled from two polypeptides, each containing one NBD and one TMD.

Contrary to ABC half-transporters, which obligatorily form homo- or heterodimers in order to gain transport activity, the functional unit of full ABC transporters is believed to be the monomer (10). This traditional view has changed over the last years. Accumulating evidence points to the existence of dimers or even higher oligomers in the case of several full transporters from different subfamilies, among them ABCB1/P-glycoprotein, ABCC1/MRP1 and ABCC7/CFTR (11-13). Oligomerization was related to the transport activity of these transporters (10).

Members of the ABCA subfamily are mostly involved in lipid transport (14). In the case of the cholesterol transporter ABCA1, Denis *et al* demonstrated that ABCA1 predominantly exists as a homotetramer (15). ABCA3 is another member of the ABC transporter subfamily A, transporting choline-phospholipids and cholesterol into lamellar bodies in alveolar epithelial type II cells (16,17). ABCA3 deficiency in humans

leads to acute respiratory distress syndrome in newborns and interstitial lung disease in children and adults (18-20).

In the present study, we investigated a possible oligomerization of ABCA3. We used a combination of classical *in vitro* biochemical methods with molecular *in vivo* techniques, i.e., bioluminescence resonance energy transfer (BRET), to demonstrate that ABCA3 predominantly exists as a homooligomer. Moreover, we showed that the arrest of ABCA3 in the endoplasmic reticulum (ER), either through drug treatment or induced by mutations in *ABCA3*, interferes with the ability of the protein's to form dimers, pointing to a novel pathomechanism in ABCA3-associated lung disease.

Materials and methods

Unless otherwise indicated, all chemicals were purchased from Sigma-Aldrich (Taufkirchen, Germany).

Antibodies. The following antibodies were used: rat anti-hemagglutinin (HA) (#11867423001; Roche, Grenzach-Wyhlen, Germany), mouse anti-GFP (#632380; Clonetech, Mountain View, USA) (for the detection of EYFP-tag, referenced as 'EYFP-antibody' throughout the manuscript), mouse anti-LAMP3 (#561924; BD Pharmingen, Heidelberg, Germany), Alexa Fluor 488 donkey anti-rat IgG (#A-21208), Alexa Fluor 555 goat anti-mouse IgG (#A-21422) (both from Thermo Fisher Scientific, Waltham, MA, USA), chicken HRP-conjugated anti-β-actin (#sc-47778; Santa Cruz Biotechnology, Inc., Heidelberg, Germany) and HRP-conjugated rabbit anti-rat IgG (#P0450; Dako, Glostrup, Denmark). For the detection of mouse primary antibodies, the Western Breeze Chemiluminescent Immunodetection system (Invitrogen, Karlsruhe, Germany) was used.

Cell culture. 293 cells (aka HEK293) were purchased from the German Collection of Microorganisms and Cell Cultures (DSMZ, Braunschweig, Germany). The cells were maintained in RPMI-1640 medium supplemented with 10% fetal bovine serum (FBS) at 37˚C with 5% CO_2. Plasmids encoding HA- and EYFP-tagged ABCA3 were constructed as previously described (21,22). The 293 cells were transfected with the pUB6-ABCA3-WT and pEYFP-ABCA3-WT vectors using ExGene 500 (Fermentas, St. Leon-Rot, Germany) according to the manufacturer's instructions. Twenty-four hours post-transfection, the selection of stable cells began by the addition of 6 μg/ml Blasticidin (Invivogen, San Diego, CA, USA) or 500 μg/ml G-418 (Roth, Karlsruhe, Germany). Single cell clones were obtained by transferring single cells into the wells of a 96-well plate. For transient transfected experiments, cells were seeded into 10 cm dishes and grown for 48 h in RPMI-1640 supplemented with 10% FBS.

Crude membrane preparation. Cells in 10 cm dishes were rinsed with phosphate-buffered saline (PBS) once and covered with ice-cold homogenization buffer [PBS supplemented with 1 mM EDTA and complete protease inhibitor cocktail (Roche)] and scraped from the dish. Subsequently, the cells were broken in a glass homogenizer with 30 strokes and sonicated on ice. The nuclei and cell debris were removed by centrifugation (700 x g, 4˚C, 10 min) and the post-nuclear supernatant was centrifuged for 1 h at 100,000 x g and 4˚C. The crude membrane fraction was resuspended in 30 μl resuspension buffer (25 mM HEPES/NaOH pH 7.0, complete protease inhibitor cocktail). The protein concentration of the post-nuclear supernatant was determined with the Bio-Rad protein assay (Bradford assay) using BSA as protein standard.

Blue native-polyacrylamide gel electrophoresis (BN-PAGE) and western blot analysis. A total of 10 μg of crude membrane lysates solubilized in 1% n-dodecyl-β-D-maltoside (DDM) or digitonin for 30 min at 37˚C were loaded onto 3-12% NativePAGE Novex Bis-Tris polyacrylamide gels (Invitrogen). Dithiothreitol (DTT) was added to the samples before solubilization as indicated. For digestion of contaminating DNA, $MgCl_2$ was added to a final concentration of 2 mM and lysates were treated with benzonase for 45 min at room temperature prior to solubilization. Following gel electrophoresis, proteins were blotted to PVDF-membranes (Millipore, Billerica, MA, USA). After transfer, the membranes were blocked with 5% skim milk in TBS-T. The membranes were incubated overnight with primary antibodies in blocking solution. After washing the membranes three times with TBS-T, HRP-conjugated secondary antibodies were applied for 1 h at room temperature. Detection was performed using ECL reagent (GE Healthcare, Freiburg, Germany).

Gel filtration. Gel filtration chromatography was performed using an ÄKTA purifier system (Amersham Biosciences, Freiburg, Germany) with a Superose 6 HR 10/30 column. A total of 200 μg of crude membrane preparations were solubilized by 1% DDM in sample buffer containing 50 mM Tris-HCl, pH 8.0 and 100 mM DTT for 30 min at room temperature. Following centrifugation at 13,000 x g for 15 min, the supernatants were injected onto the column, which was equilibrated with 2.5 column volumes with running buffer (50 mM Tris-HCl, pH 7.4, 150 mM NaCl, 1 mM DTT and 0.1% DDM). The eluate was collected in fractions of 1 ml each, concentrated using Amicon Ultra columns 50 K (Millipore) according to the manufacturers' instructions, and subjected to sodium dodecyl sulfate-polyacrylamide gel electrophoresis (SDS-PAGE) or BN-PAGE and western blot analysis as described above. The column was standardized with the Gel Filtration Calibration kit LMW (GE Healthcare) and the western blot signal was quantified by measuring the intensity using GelAnalyzer 2010a software (Lazar Software).

Co-immunoprecipitation. Forty-eight hours after transfection with pUB6-ABCA3-WT-HA, pEYFP-ABCA3-WT or both vectors, the 293 cells were lysed in lysis buffer [50 mM Tris-HCl, 150 mM NaCl, 1 mM EDTA, 1% (v/v) Triton X-100, pH 7.4] supplemented with complete protease inhibitor. Clarified lysates were immunoprecipitated using anti-HA antibody coupled with magnetic Dynabeads (Invitrogen) according to the manufacturer's instructions. Precipitated proteins were eluted with elution buffer (200 mM Glycin and 0.01% (v/v) Tween-20, pH 2.8). 4X LDS buffer (Invitrogen) and DTT (50 mM) were added and the solution was incubated for 10 min at 70˚C. Samples were then separated by SDS-PAGE using NuPAGE Mini 3-8% Tris-Acetate gels (Invitrogen). Following gel electrophoresis, proteins were blotted to PVDF membranes (Millipore) and blocked with 5% skim milk in TBS-T. Following overnight incubation with

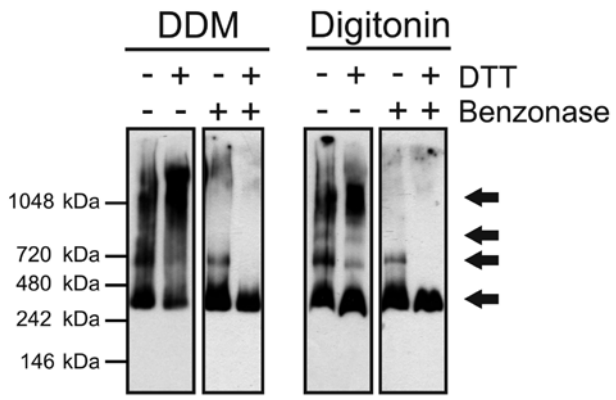

Figure 1. Analysis of oligomeric ABCA3 complexes by blue native PAGE (BN-PAGE). Crude membrane preparations from transiently transfected 293 cells were dissolved in n-dodecyl-β-D-maltoside (DDM) or Digitonin at 37˚C for 30 min and separated on 3-12% NativePAGE Novex Bis-Tris Gel under native conditions. Western blot analysis was used to detect specific HA-tags. At least four different fragments are visible (black arrows), with the smallest fragment, indicating the monomeric form, showing the strongest signal. Treatment with 50 mM dithiothreitol (DTT) led to an accumulation of the highest form at approximately 1,000 kDa (DDM) and in the case of digitonin of the highest and lowest monomeric form (right panel). An additional benzonase endonuclease treatment requires the use of $MgCl_2$ in a final concentration of 2 mM and 2 units benzonase/μl of sample and incubation for 30 min at room temperature. The monomeric and dimeric fragments are also visible. Treatment with DTT causes an accumulation of the monomeric state.

anti-HA or anti-EYFP antibody, the membranes were washed and incubated with HRP-conjugated secondary antibodies for 1 h or 30 min, respectively. The detection was performed with ECL reagent (GE Healthcare) or, in the case of the EYFP-antibody, with secondary antibody solution (Invitrogen). Membranes were stripped with Restore buffer (Pierce/Thermo Fisher Scientific) and re-stained with the complementary antibody (anti-EYFP or anti-HA).

BRET. Wild-type and mutant hABCA3 (NM_001089.2), and phenylalanine hydroxylase (PAH, U49897.1) were introduced into pDONR™221 (Invitrogen) by recombinational cloning according to the manufacturer's instructions. Expression clones coding for N- and C-terminal fusion proteins with an improved version of YFP (EYFP) or *Renilla* luciferase (Rluc) were generated by the recombination of pDONRTM221 entry clones with the respective destination vectors.

The interaction of proteins in living cells was analyzed by BRET as previously described (23). BRET was performed in living 293 cells. Binary interactions were tested in all four possible combinations of two proteins of interest either fused to Rluc (energy donor) or EYFP (energy acceptor). Cells were co-transfected with a total of 0.8 μg of DNA at an acceptor to donor ratio of 3:1. BRET saturation experiments were performed to distinguish a true positive interaction from bystander BRET resulting from random collision. Cells were co-transfected at increasing acceptor to donor ratios with a total of 2 μg DNA. All combinations were tested in three independent experiments. The cells were incubated at 30˚C or 37˚C, respectively. Following 48 h of incubation, coelenterazine (15 μM, PJK) was added to the living cells and light emission was collected in a 96-well microplate luminometer (PHERAstar FS, BMG LABTECH) for 10 sec at 475 nm (Rluc signal) and 535 nm (EYFP signal). The BRET ratio was calculated based on $R = I_A/I_D$ - *cf*, where R is the BRET ratio, I_A is the intensity of light emission at 535 nm, I_D is the intensity of light emission at 475 nm, and *cf* is a correction factor ($BRET_{control}/Rluc_{control}$) with the control being the co-transfection of donor fusion-proteins with EYFP in the absence of a second protein of interest. In addition, the background of a noDNA control was subtracted, general BRET efficiency was tested by a EYFP-Rluc fusion protein, and assay performance was evaluated using a standard protein interaction pair (b-Jun and b-Fos). Relative affinities were calculated using the non-linear regression model $Y = BRET_{max}$ x ($X/BRET_{50} + X$), where $BRET_{max}$ is the maximal BRET ratio and $BRET_{50}$ is the acceptor to donor ratio required to reach half-maximal BRET. For additional Brefeldin A (BFA) treatment, the cells were treated after 24 h of incubation with BFA (10 μg/ml in ethanol) for 24 h. Cells treated with ethanol were used as the vehicle control, and untreated cells were used as negative controls. BRET measurement was then performed as described above.

Statistic analysis. Comparisons of multiple groups were carried out using one-way repeated measure ANOVAs with Tukey's post hoc test. The results are presented as mean ± SEM of a minimum of three different experiments. P-values of <0.05 were considered to indicate statistically significant differences. For saturation experiments, nonlinear regression was applied. All tests were performed using GraphPad Prism 5.0 (GraphPad Software, La Jolla, CA, USA).

Results

Heterlogous expression of ABCA3 protein. Transfection of the 293 cells with the pUB6-ABCA3-WT and pEYFP-ABCA3-WT vectors resulted in the robust expression of ABCA3, as detected by immunofluorescence and western blot analysis. Both HA- and EYFP-tagged ABCA3-WT were mainly localized in LAMP3-positive intracellular vesicles in the 293 cells and yielded two protein bands of approximately 220/190 and 180/150 kDa for EYFP- and HA-tagged ABCA3, respectively (data not shown). These features are in concordance with the findings of a previous study (24).

Non-ionic detergent extraction and BN-PAGE analysis of human ABCA3. Following solubilization, proteins were separated on a 3-12% native PAGE Bis-Tris polyacrylamide gel in the presence of DDM or digitonin (Fig. 1). BN-PAGE revealed roughly similar patterns of protein bands in both of the solubilizates with the prevalence of one major band with the size of the presumed monomer, particularly in the case of DDM treatment. Additionally, next to the monomer, three higher molecular mass forms were detectable, which likely represent dimeric, trimeric and tetrameric ABCA3. The observed molecular masses were 374.2±13.8 kDa for the monomer, 631.0±11.1 kDa for the dimer, 864.0±34.4 kDa for the trimer/tetramer and 1213.8±89.5 kDa for a higher oligomeric complex (Table I). The bands observed in the case of the digitonin-treated samples (right panel) were similar in mass (347.8±44.8 kDa monomer, 610.0±24.5 kDa dimer, 796.5±24.7 kDa trimer/tetramer, 1079±26.9 kDa higher oligomer). The monomers (45%) and

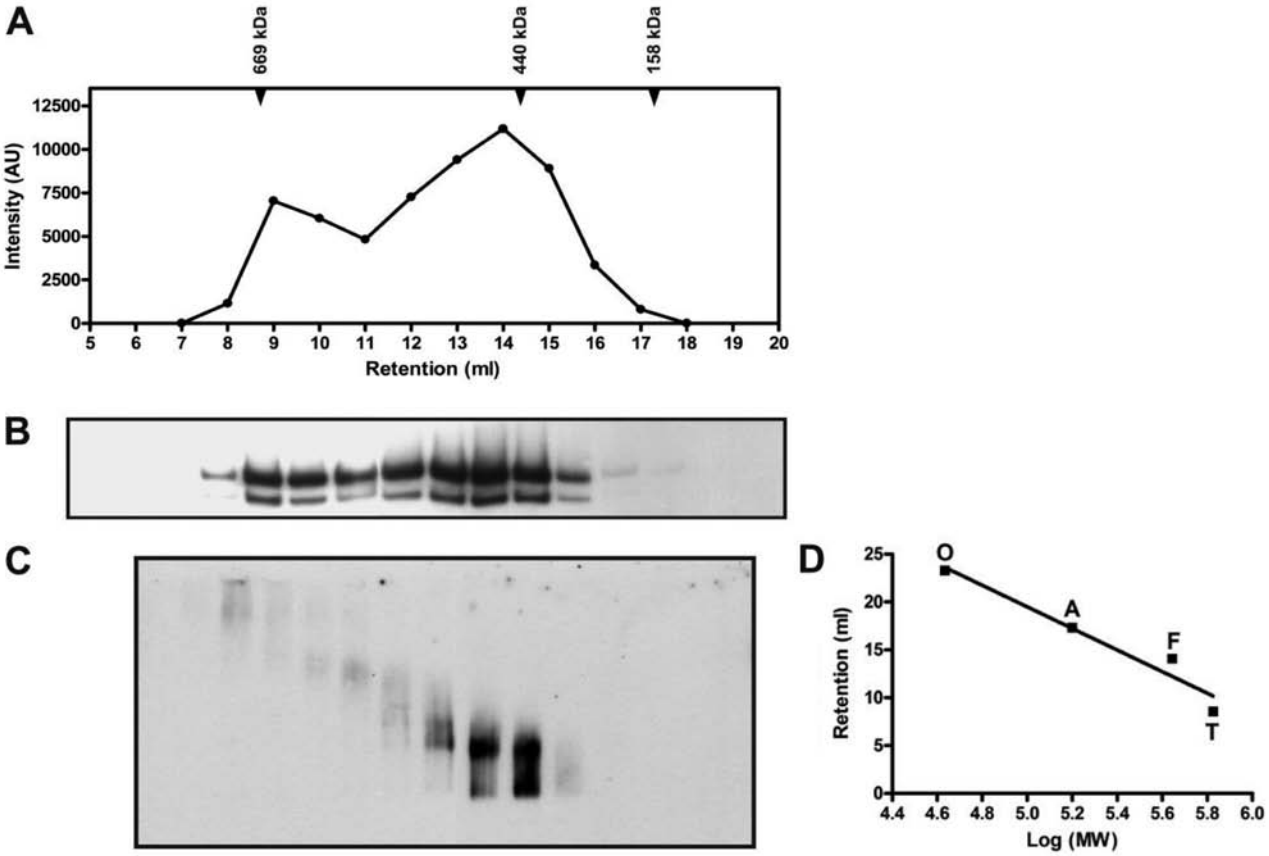

Figure 2. Analysis of the oligomeric state of ABCA3 by gel filtration chromatography. Size exclusion chromatography of ABCA3 was performed following solubilisation of 200 μg crude membrane preparation from transiently transfected 293 treated with 1% n-dodecyl-β-D-maltoside (DDM) over a Superose HR60 column on an ÄKTA purifier system using a flow rate of 0,4 ml/min. The fractions containing HA-tagged ABCA3 were collected and concentrated with Amicon Ultra centrifugal filters for (B) sodium dodecyl sulfate-polyacrylamide gel electrophoresis (SDS-PAGE) and (C) blue native PAGE (BN-PAGE) both followed by western blot analysis. After SDS-PAGE the HA-signal in each fraction was quantified by measuring the intensity of the western blot analysis using GelAnalyzer 2010a software and plotted against the retention volume (A). Retention time of marker protein thyroglobulin (699 kDa), ferritin (440 kDa) and aldolase (158 kDa) in DDM were marked. BN-PAGE shows higher oligomers in early fractions (fraction 8 and 9) and dimeric (fraction 13-15) and monomeric (fraction 14-16) ABCA3 forms in the later eluted fractions. (D) Estimation of molecular weight is performed by the floating of protein markers thyroglobulin (T), ferritin (F), aldolase (A) and ovalbumin (O) in parallel and equivalent gradients.

tetramers (30%) were the most determined forms, followed by 20% dimers and 5% trimers. Treatment with DTT, i.e., reduction of disulphide bonds, led to the accumulation of high molecular weight forms in the DDM- and digitonin-solubilized samples. In the case of digitonin-treated samples, the band corresponding to the monomer was more pronounced after DDT treatment. Since complete dissociation to monomers was not achieved, benzonase endonuclease digestion was performed to avoid protein streaking caused by a high DNA content in samples. Benzonase treatment resulted in the almost complete absence of high molecular weight forms, remaining only the bands putatively corresponding to monomeric and dimeric ABCA3. In the cells treated with DTT and benzonase, eventually all forms other than the supposed monomer were absent.

Gel filtration chromatography analysis of human ABCA3. After gel filtration chromatography, ABCA3 was found exclusively in fractions 8-17 in following SDS-PAGE (Fig. 2). When the western blot signal was quantified by measuring the intensity plotted against the retention volume (Fig. 2A), it was apparent that two peaks were eluted, wherein the second peak was more intense. The typical pattern with two ABCA3 bands remained in SDS-PAGE (Fig. 2B).

When BN-PAGE subsequent to gel filtration was used to analyze the oligomeric pattern, we found complex structures in the early-eluted fractions 8 and 9 (Fig. 2C). Smaller oligomeric forms supposed to represent ABCA3 tetramers, trimers or dimers were found in fractions 10-15. Molecular weights estimated by comparison with marker proteins are given in Table I. The presumed monomeric form which has an estimated molecular mass of 392.5±19.1 kDa was also present in fractions 14-16.

Co-immunoprecipitation of human ABCA3. To further verify ABCA3 homooligomerization, we performed co-immunoprecipitation with two differentially tagged ABCA3 fusion proteins. For this purpose, EYFP-tagged ABCA3 was transiently transfected into 293 cells that did or did not express stable HA-epitope-tagged ABCA3. Following transfection, cell lysates were prepared and co-immunoprecipitation was performed with anti-HA antibody, followed by western blot analysis using both anti-HA and anti-EYFP antibodies (Fig. 3). The EYFP-ABCA3 fusion protein could be immunoprecipitated with the anti-HA antibody only in cells that were co-transfected with both tagged proteins. Thus, the oligomeric state of human ABCA3 is as least dimeric when expressed in 293 cells.

Table I. Overview of ABCA3 forms identified by different methods.

Method	Form	Estimated molecular weight (kDa)	Estimated true molecular weight (kDa)[a]	Percentage
SDS-PAGE in literature (17,22)	Processed monomer	190		
	Unprocessed monomer	150		
SDS-PAGE	Processed monomer	165.5±12.4		
	Unprocessed monomer	192.5±10.5		
BN-PAGE				
Detergent				
DDM	Monomer	374.2±13.8	207.9	45
	Dimer	631.0±11.1	350.6	25
	Trimer	894.0±34.4	496.7	2
	Tetramer	1214±89.5	674.3	28
Digitonin	Monomer	347.8±44.8	193.2	44
	Dimer	610.0±24.5	338.9	16
	Trimer	796.5±24.7	442.5	7
	Tetramer	1079±26.9	599.4	33
Gel filtration	Comparison with standard proteins			
	Monomer	247.3		
	Dimer	310.8		
	Trimer	456.0		
	Tetramer	774.5		
	SDS-PAGE			
	Processed monomer	150.2±14.4		
	Unprocessed monomer	167.1±15.0		
	BN-PAGE			
	Monomer	392.5±19.1	218.1	
	Dimer	602.5±35.5	334.7	
	Trimer	951.3±105	528.5	
	Tetramer	1579±196	876.9	

[a]Using an average ratio of CBB-protein-complex to protein of 1.8 (see Discussion). SDS-PAGE, sodium dodecyl sulfate-polyacrylamide gel electrophoresis; BN-PAGE, blue native PAGE; CBB, Coomassie brilliant blue.

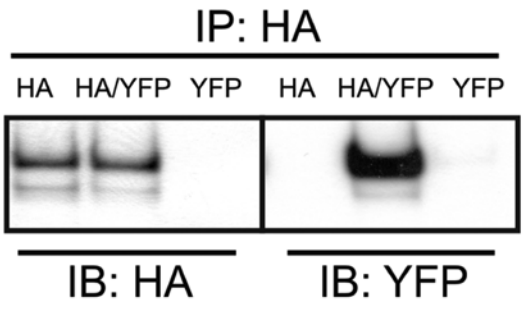

Figure 3. Co-immunoprecipitation of differently tagged ABCA3 proteins. C-terminally HA- or EYFP-tagged forms of human ABCA3 were expressed individually (HA, EYFP) or co-expressed (HA/EYFP) in HEK293 cells. Cell lysates were immunoprecipitated (IP) using anti-HA antibody, resolved by sodium dodecyl sulfate-polyacrylamide gel electrophoresis (SDS-PAGE) and immunoblotted (IB) against anti-HA and anti-EYFP.

BRET assay confirms the homooligomerization of human ABCA3 in vivo. To confirm the homooligomerization of ABCA3 in living cells, we performed BRET analyses. Cells were co-transfected with ABCA3 carrying N- or C-terminal tags of Rluc or EYFP, respectively, in four possible combinations (Fig. 4A and B). The correct cellular localization of the N- and C-terminally tag fusion proteins was verified by immunofluorescence microscopy (data not shown). Two out of eight combinations resulted in BRET ratios above the background level; however, BRET ratios did not exceed the method-specific threshold for a positive protein-protein interaction of 0.094. Due to better folding characteristics at lower temperatures (25), we performed BRET experiments at 30˚C. Under these conditions, the respective combinations resulted in BRET ratios above the method-specific threshold, indicating a homooligomerization of ABCA3. To further substantiate homomeric interaction of ABCA3 in living cells, we performed BRET saturation experiments (Fig. 4C and D). For specific protein-protein interactions, such as the formation of homooligomeric states, a sequential increase in the ratio of proteins carrying the EYFP tag over proteins carrying the Rluc tag results in hyperbolic behavior of the BRET ratios (26). In addition, a relative binding affinity index can be determined by use of the EYFP to Rluc ratio

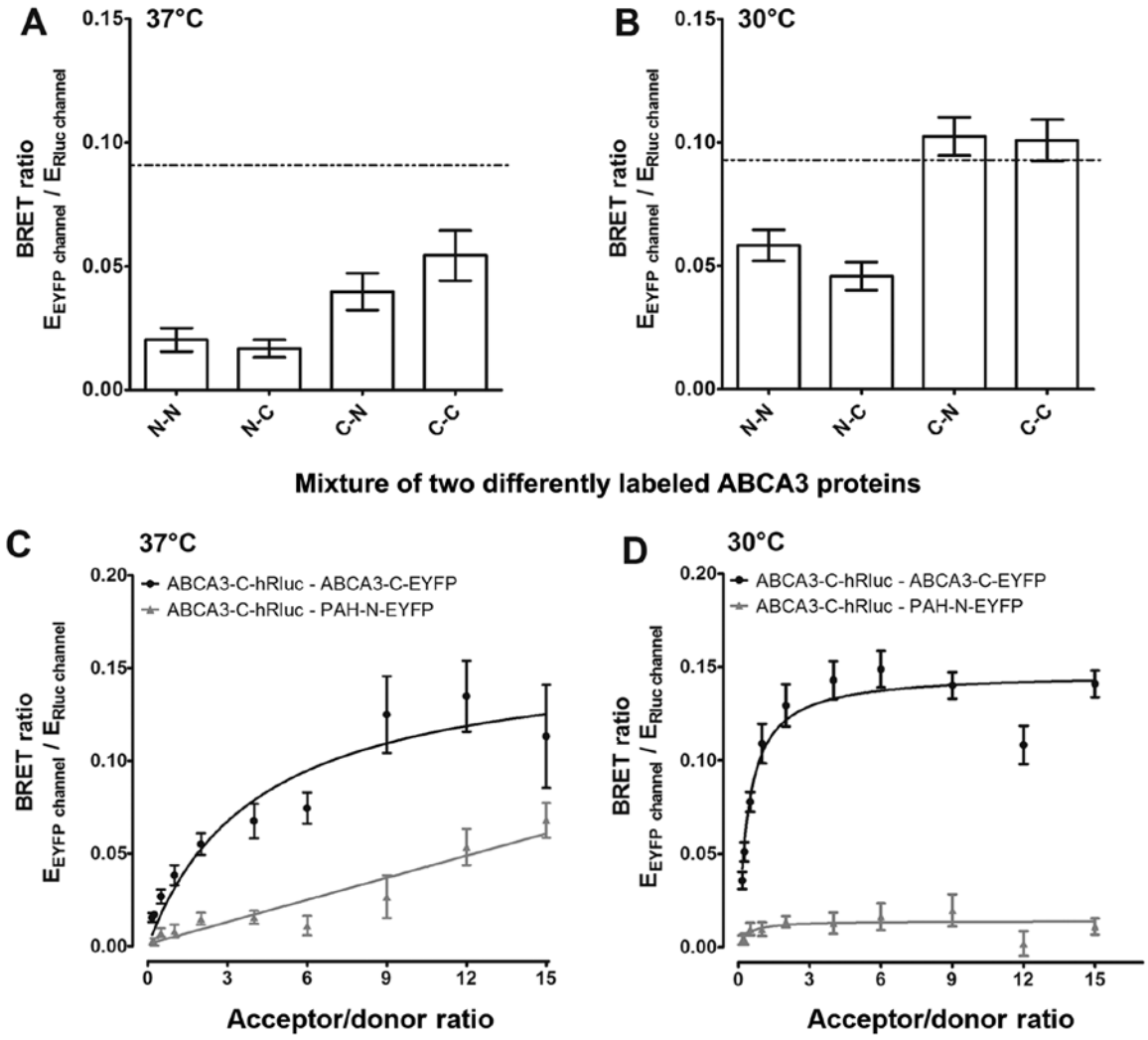

Figure 4. Detection of ABCA3 homodimerization by bioluminescence resonance energy transfer (BRET) assay in living cells. (A and B) Interaction of ABCA3 analyzed by BRET at 37˚C and 30˚C. Experiments were performed in four possible combinations of ABCA3 with N-terminal and C-terminal tags of Rluc or YFP. BRET ratios are presented as the means ± SEM of n=3-4 independent experiments. The dashed line depicts the method specific threshold for a positive protein-protein interaction of 0.094. (C and D) BRET saturation experiments for ABCA3-ABCA3 and ABCA3-PAH (control) determining the acceptor to donor ratio at half-maximal BRET ratio ($BRET_{50}$) as a measure for the relative binding affinity. Experiments were performed with C-C terminal tags and BRET ratios as a function of the acceptor to donor ratio are shown. Data are presented as the means of n=3 experiments.

(acceptor/donor ratio) at half-maximal BRET ($BRET_{50}$). Co-expression of homomeric protein pairs with C-terminal tags resulted in hyperbolic BRET curves with a $BRET_{50}$ value of 4,091 at 37˚C and 0,415 at 30˚C. These data confirm the homooligomerization of ABCA3 at 30˚C and at physiological conditions (37˚C), with higher affinities of oligomer formation at 30˚C. As a negative control, the co-transfection of ABCA3 with PAH resulted in a curve best fitted by linear regression, which is indicative for bystander BRET due to random collision.

Determination of the localization of the ABCA3-ABCA3 interaction. To explore the intracellular localization of the ABCA3 homooligomerization we used BFA treatment. BFA inhibits the transportation of proteins from the ER to the Golgi apparatus, resulting in protein accumulation in the ER (27). The cells were treated with BFA (10 μg/ml) or the vehicle (ethanol) for 24 h prior to BRET measurement, which was done at 30˚C (Fig. 5). Treatment with BFA resulted in a significantly lower BRET ratio for the ABCA3-ABCA3 interaction compared to the negative control, while no significant difference was noted in the case of the vehicle control. This observation suggested that the ABCA3-ABCA3 interaction (and thus the formation of oligomers) takes place in a post-ER compartment.

The mistrafficking mutation p.Q215K interferes with the ABCA3-ABCA3 interaction. To determine whether ABCA3 mutations disrupt ABCA3 oligomer formation, BRET experiments were performed for the wild-type protein compared to four different clinically relevant mutations. All experiments were performed at 37˚C and 30˚C. While in three of four tested mutations (R280C, R288K and S693L) BRET ratios were nearly similar to wild-type ABCA3 for all configurations tested, in the case of ABCA3-Q215K, BRET ratios were hardly detectable (Fig. 6). To confirm this, we again performed BRET saturation experiments (Fig. 7). Low BRET ratios and a lack of hyperbolic behavior of the BRET ratios confirmed that Q215K leads to perturbation of the ABCA3 homooligomerization.

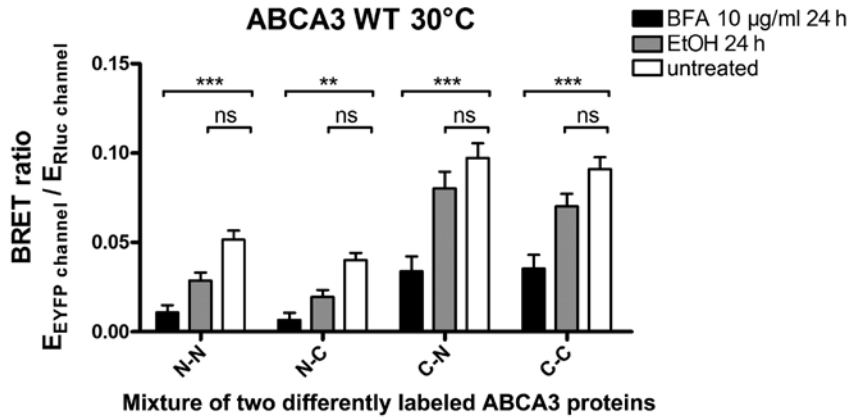

Figure 5. Bioluminescence resonance energy transfer (BRET) measurements after BFA treatment. Experiments were performed in four possible combinations of ABCA3 with N-terminal and C-terminal tags of Rluc or YFP for one-point-measurements with additional BFA (10 μg/ml) treatment, or EtOH treatment only (control), at 30˚C. Results are expressed as the means ± SEM of three experiments (**P<0.01 and ***P<0.001, ns, not significant).

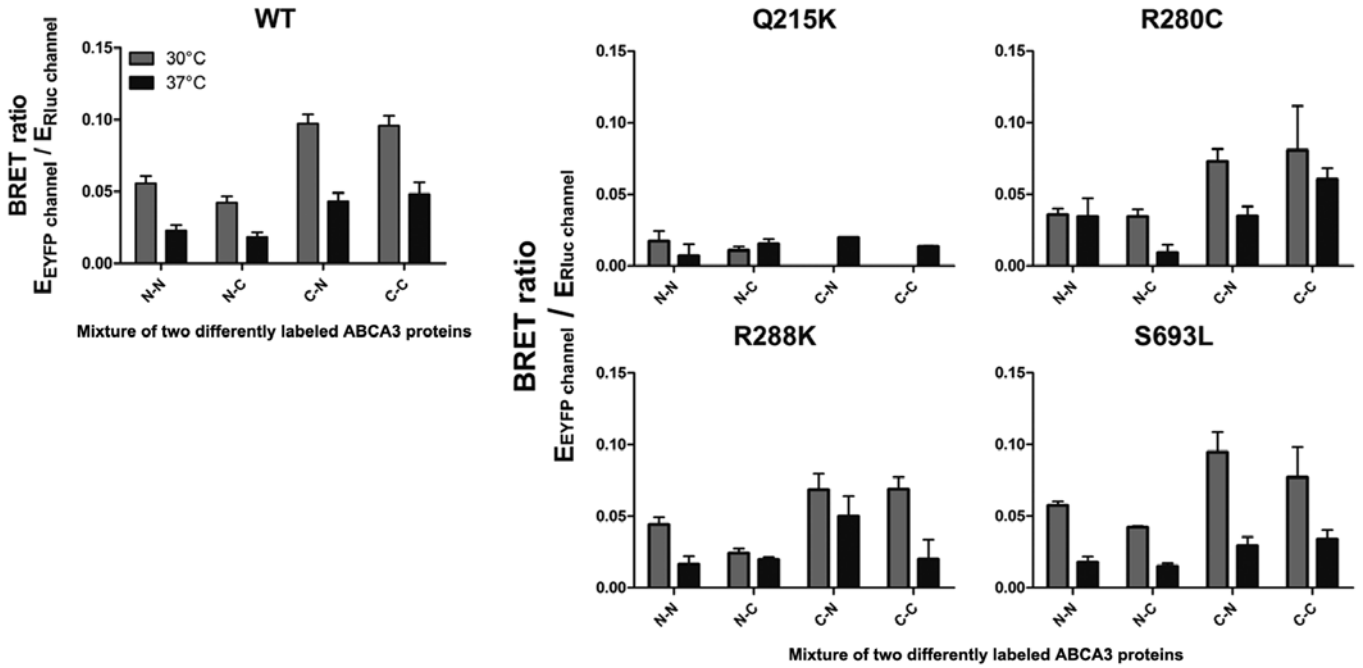

Figure 6. Homodimerization analysis of wild-type and mutated ABCA3 proteins by bioluminescence resonance energy transfer (BRET) assay. Experiments were performed in four possible combinations of ABCA3 wild-type compared to mutant ABCA3 (Q215K, R280C, R288K and S693) with N-terminal and C-terminal tags of Rluc or YFP, at two different incubation temperatures (grey bars, 30˚C; black bars, 37˚C). All the results are expressed as means ± SEM of three experiments.

Since p.Q215K leads to the arrest of ABCA3 in the ER (22), this result corroborates the assumption that ABCA3-ABCA3 interaction takes place in a post-ER compartment.

Discussion

In this study, using different complementary approaches, we demonstrate that the lipid transporter ABCA3 forms dimers and possibly also higher oligomers. Using BRET technology, an independent method to assess protein-protein interactions in living cells avoiding detergent solubilization, we demonstrate that homooligomerization occurs *in vivo*. Moreover, we show that mutations in ABCA3 can negatively affect oligomerization. Since homooligomerization can be expected to be of functional significance, these findings point to a new level of the regulation of ABCA3 function. Our data may also introduce the perturbation of oligomer formation as a new mechanism by which mutations interfere with ABCA3 function.

To the best of our knowledge, the question of whether ABCA3 forms oligomers has not been addressed by any study to date. However, as stated above, oligomerization has been demonstrated for the lipid transporter ABCA1 (15,28). Given the close association of these two subclass A transporters, it does not come as a surprise that ABCA3 behaves in a similar way and forms dimers and higher oligomers *in vitro* and also *in vivo*. It therefore adds to the growing list of ABC transporters for which oligomerization has been demonstrated, suggesting a functional relevance of oligomerization.

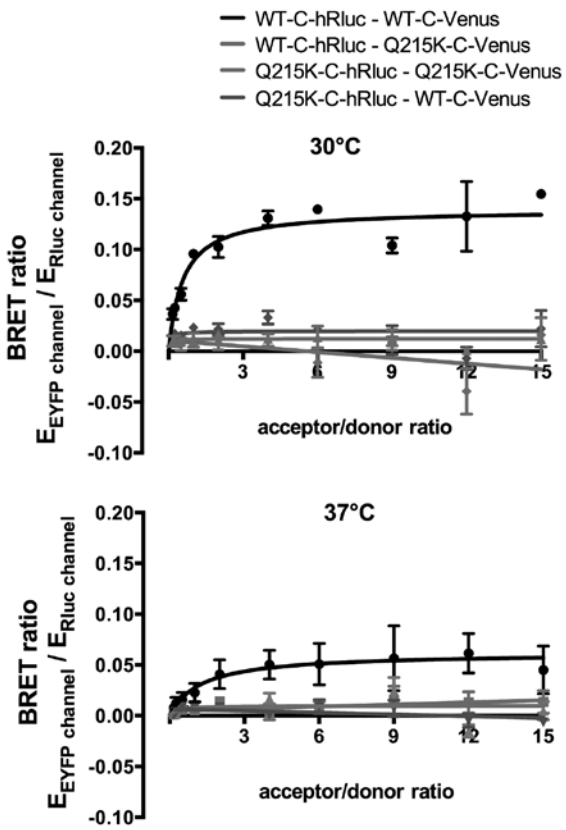

Figure 7. BRET Saturation assay with ABCA3-WT and ABCA3-Q215K. BRET saturation experiments were performed for WT-C-hRluc + WT-C-EYFP (black line with filled circles), WT-C-hRluc + Q215K-C-EYFP (grey line), Q215K-C-hRluc + Q215K-C-EYFP (grey line with diamonds) and Q215K-C-hRluc + WT-C-EYFP (dark grey line). Nonlinear regression model was applied. Data are given as means ± SEM of n=3 replicates.

We aimed to reliably establish the homooligomerization of ABCA3 by using various approaches complementing each other. While co-immunoprecipation detects ABCA3-ABCA3 interaction, BN-PAGE can be used to visualize the oligomeric states of the protein. In addition, we used gel filtration chromatography as an alternative approach for quantifying the molecular masses of oligomeric forms. Since all these biochemical methods may yield false-positive results due to artifacts of the extraction process, the analysis of protein-protein interaction by BRET circumvents this issue and permits the measurement of interactions *in vivo*.

The accurate determination of the molecular mass and thereby the oligomeric state of membrane proteins is a challenging task. BN-PAGE is widely used for the analysis of the composition, oligomeric state and molecular mass of non-dissociated membrane protein complexes. However, when determining molecular masses of proteins from BN-PAGE, one must take into account that membrane proteins bind large amounts of Coomassie brilliant blue (CBB) dye. Bound dye adds to the apparent masses of the proteins and results in an overestimation. To address this issue, Heuberger *et al* established that taking into account an average ratio of CBB-protein-complex to pure protein of approximately 1.8, molecular masses deduced from BN-PAGE via a soluble marker calibration curve can be converted to provide a good estimate of the true molecular mass (29). Using this correction, we identified oligomeric ABCA3 forms including dimers, trimers and tetramers. The molecular masses deduced from BN-PAGE are in good agreement with those estimated from gel filtration chromatography with subsequent BN-PAGE (Table I). Size estimation in gel filtration with only standard proteins (thyroglobulin, ferritin and aldolase) shows the same deviations as ready to use markers in BN-PAGE owing to the fact that these proteins are cytosolic and have a different running behavior in the column than membrane proteins.

Using BRET, we demonstrated ABCA3-ABCA3 interaction *in vivo*. In all experiments, interaction affinity was higher at lower temperatures. This may be explained by more efficient folding of the large ABCA3 protein at lower temperatures, when overexpressed in cells (25,30). Since the C-C combination showed the highest BRET ratio in our measurements (Fig. 4), we conclude that the C-termini of ABCA3 are in close proximity. The C-terminal interaction of ABCA3 is likely to be of functional relevance, since similar C-terminal interaction sites were identified for ABCA1 and ABCC7/CFTR (31,32).

How the oligomerization of ABC transporters is related to their transport activities is still a matter of debate and it is possible that both, monomeric and oligimeric, forms co-exist and there might be a dynamic process of formation and dissociation that can influence the substrate binding affinity and may function as another level of transporter regulation (10). To this end, Trompier *et al* showed that ABCA1 tetramers are formed upon binding of ATP, while the transporter is present predominantly as a homodimer (28). This scenario, which may also apply to ABCA3, implies that the transition of dimers into higher order structures is an integral part of the protein's catalytic cycle and thus crucially required for its activity. The assumption that oligomerization is a prerequisite for transport activity also implies possible detrimental effects of mutations affecting oligomerization on ABCA3 function. It is thus important to determine whether ABCA3 mutations that are found in patients suffering from ABCA3-assosciated lung disease have any impact on its oligomerization. Among the mutations we tested, three mutations (p.R280C, p.R288K and p.S693L) showed BRET ratios comparable to the wild-type protein, while in the case of p.Q215K the BRET signal was almost absent.

We showed that the ABCA3 mutation p.Q215K, which was associated with the arrest of the protein in the ER, practically abolished oligomerization. While this is consistent with the view that oligomerization is a prerequisite for export from the ER, one could also argue that ER arrest induced by the p.Q215K mutation blocks oligomerization, which is in line with diminished oligomer formation caused by BFA treatment. However, it is also conceivable that BFA treatment directly affects the oligomerization of ABCA3 by blocking the ER to Golgi transport. Consecutive protein accumulation may hamper the ABCA3-ABCA3 interaction required for oligomerization. In addition, ABCA1 dimerization was shown to take place in the ER (28). Thus, our data are consistent with the notion that ABCA3 oligomerization takes place in the ER and that the misfolding of ABCA3-p.Q215K abrogates protein-protein interaction needed for formation of oligomers and subsequent ER export.

Taken together, the findings of the present study demonstrate that ABCA3 monomers form dimers and to a lesser

extent, also higher oligomers. We further demonstrate that the oligomerization and trafficking of ABCA3 are mutually dependent, and that mutations can interfere with this process. We have thus unraveled a potential novel molecular mechanism for ABCA3-related interstitial lung disease.

Acknowledgements

We would like to thank Claudia Bräu-Heberger, Kathrin Schiffl and Andrea Schams for their excellent technical assistance. This study was supported by a grant from the Deutsche Forschungsgemeinschaft to M.G. (GR 970/8-1).

References

1. Wilkens S: Structure and mechanism of ABC transporters. F1000Prime Rep 7: 14, 2015.
2. Dean M, Hamon Y and Chimini G: The human ATP-binding cassette (ABC) transporter superfamily. J Lipid Res 42: 1007-1017, 2001.
3. Bodzioch M, Orsó E, Klucken J, Langmann T, Böttcher A, Diederich W, Drobnik W, Barlage S, Büchler C, Porsch-Ozcürümez M, *et al*: The gene encoding ATP-binding cassette transporter 1 is mutated in Tangier disease. Nat Genet 22: 347-351, 1999.
4. Brooks-Wilson A, Marcil M, Clee SM, Zhang LH, Roomp K, van Dam M, Yu L, Brewer C, Collins JA, Molhuizen HO, *et al*: Mutations in ABC1 in Tangier disease and familial high-density lipoprotein deficiency. Nat Genet 22: 336-345, 1999.
5. Allikmets R, Singh N, Sun H, Shroyer NF, Hutchinson A, Chidambaram , Gerrard B, Baird L, Stauffer D, Peiffer A, *et al*: A photoreceptor cell-specific ATP-binding transporter gene (ABCR) is mutated in recessive Stargardt macular dystrophy. Nat Genet 15: 236-246, 1997.
6. Bergen AA, Plomp AS, Schuurman EJ, Terry S, Breuning M, Dauwerse H, Swart J, Kool M, van Soest S, Baas F, *et al*: Mutations in ABCC6 cause pseudoxanthoma elasticum. Nat Genet 25: 228-231, 2000.
7. Riordan JR, Rommens JM, Kerem B, Alon N, Rozmahel R, Grzelczak Z, Zielenski J, Lok S, Plavsic N, Chou JL, *et al*: Identification of the cystic fibrosis gene: Cloning and characterization of complementary DNA. Science 245: 1066-1073, 1989.
8. Kartner N, Riordan JR and Ling V: Cell surface P-glycoprotein associated with multidrug resistance in mammalian cell lines. Science 221: 1285-1288, 1983.
9. Cole SP: Multidrug resistance protein 1 (MRP1, ABCC1), a 'multitasking' ATP-binding cassette (ABC) transporter. J Biol Chem 289: 30880-30888, 2014.
10. Mo W and Zhang JT: Oligomerization of human ATP-binding cassette transporters and its potential significance in human disease. Expert Opin Drug Metab Toxicol 5: 1049-1063, 2009.
11. Jetté L, Potier M and Béliveau R: P-glycoprotein is a dimer in the kidney and brain capillary membranes: Effect of cyclosporin A and SDZ-PSC 833. Biochemistry 36: 13929-13937, 1997.
12. Soszyński M, Kałuzna A, Rychlik B, Sokal A and Bartosz G: Radiation inactivation suggests that human multidrug resistance-associated protein 1 occurs as a dimer in the human erythrocyte membrane. Arch Biochem Biophys 354: 311-316, 1998.
13. Ramjeesingh M, Kidd JF, Huan LJ, Wang Y and Bear CE: Dimeric cystic fibrosis transmembrane conductance regulator exists in the plasma membrane. Biochem J 374: 793-797, 2003.
14. Albrecht C and Viturro E: The ABCA subfamily - gene and protein structures, functions and associated hereditary diseases. Pflugers Arch 453: 581-589, 2007.
15. Denis M, Haidar B, Marcil M, Bouvier M, Krimbou L and Genest J: Characterization of oligomeric human ATP binding cassette transporter A1. Potential implications for determining the structure of nascent high density lipoprotein particles. J Biol Chem 279: 41529-41536, 2004.
16. Ban N, Matsumura Y, Sakai H, Takanezawa Y, Sasaki M, Arai H and Inagaki N: ABCA3 as a lipid transporter in pulmonary surfactant biogenesis. J Biol Chem 282: 9628-9634, 2007.
17. Matsumura Y, Sakai H, Sasaki M, Ban N and Inagaki N: ABCA3-mediated choline-phospholipids uptake into intracellular vesicles in A549 cells. FEBS Lett 581: 3139-3144, 2007.
18. Shulenin S, Nogee LM, Annilo T, Wert SE, Whitsett JA and Dean M: ABCA3 gene mutations in newborns with fatal surfactant deficiency. N Engl J Med 350: 1296-1303, 2004.
19. Bullard JE, Wert SE, Whitsett JA, Dean M and Nogee LM: ABCA3 mutations associated with pediatric interstitial lung disease. Am J Respir Crit Care Med 172: 1026-1031, 2005.
20. Campo I, Zorzetto M, Mariani F, Kadija Z, Morbini P, Dore R, Kaltenborn E, Frixel S, Zarbock R, Liebisch G, *et al*: A large kindred of pulmonary fibrosis associated with a novel ABCA3 gene variant. Respir Res 15: 43, 2014.
21. Weichert N, Kaltenborn E, Hector A, Woischnik M, Schams A, Holzinger A, Kern S and Griese M: Some ABCA3 mutations elevate ER stress and initiate apoptosis of lung epithelial cells. Respir Res 12: 4, 2011.
22. Engelbrecht S, Kaltenborn E, Griese M and Kern S: The surfactant lipid transporter ABCA3 is N-terminally cleaved inside LAMP3-positive vesicles. FEBS Lett 584: 4306-4312, 2010.
23. Gersting SW, Lotz-Havla AS and Muntau AC: Bioluminescence resonance energy transfer: An emerging tool for the detection of protein-protein interaction in living cells. Methods Mol Biol 815: 253-263, 2012.
24. Matsumura Y, Ban N, Ueda K and Inagaki N: Characterization and classification of ATP-binding cassette transporter ABCA3 mutants in fatal surfactant deficiency. J Biol Chem 281: 34503-34514, 2006.
25. Bischof JC and He X: Thermal stability of proteins. Ann NY Acad Sci 1066: 12-33, 2005.
26. Hamdan FF, Percherancier Y, Breton B and Bouvier M: Monitoring protein-protein interactions in living cells by bioluminescence resonance energy transfer (BRET). Curr Protoc Neurosci: Chapter 5, Unit 5.23, 2006.
27. Nylander S and Kalies I: Brefeldin A, but not monensin, completely blocks CD69 expression on mouse lymphocytes: Efficacy of inhibitors of protein secretion in protocols for intracellular cytokine staining by flow cytometry. J Immunol Methods 224: 69-76, 1999.
28. Trompier D, Alibert M, Davanture S, Hamon Y, Pierres M and Chimini G: Transition from dimers to higher oligomeric forms occurs during the ATPase cycle of the ABCA1 transporter. J Biol Chem 281: 20283-20290, 2006.
29. Heuberger EH, Veenhoff LM, Duurkens RH, Friesen RH and Poolman B: Oligomeric state of membrane transport proteins analyzed with blue native electrophoresis and analytical ultracentrifugation. J Mol Biol 317: 591-600, 2002.
30. Matsumoto N, Tamura S, Furuki S, Miyata N, Moser A, Shimozawa N, Moser HW, Suzuki Y, Kondo N and Fujiki Y: Mutations in novel peroxin gene PEX26 that cause peroxisome-biogenesis disorders of complementation group 8 provide a genotype-phenotype correlation. Am J Hum Genet 73: 233-246, 2003.
31. Fitzgerald ML, Okuhira K, Short GF III, Manning JJ, Bell SA and Freeman MW: ATP-binding cassette transporter A1 contains a novel C-terminal VFVNFA motif that is required for its cholesterol efflux and ApoA-I binding activities. J Biol Chem 279: 48477-48485, 2004.
32. Wang S, Yue H, Derin RB, Guggino WB and Li M: Accessory protein facilitated CFTR-CFTR interaction, a molecular mechanism to potentiate the chloride channel activity. Cell 103: 169-179, 2000.